FINAL TECHNICAL REPORT

NASA RESEARCH GRANT NGL 40-002-042

Introduction

This report will summarize all reseach activity supported in whole or in part by grant NGL 40-002-042, Properties and Application of Solid State Materials at Sub-Millimeter Frequencies, during the entire grant period, November 1966 through June 1973. This research is subdivided into five major areas: early far infrared Fourier spectroscopy; studies of the antiferromagnetic resonance line in MnF_2 at millimeter wavelengths; numerical solution of the equations of motion of a general two-sublattice antiferromagnet; later Fourier spectroscopy; study of antiferromagnetic resonance line in NiO powder, resonance investigations of several indium thisospinels at millimeter wavelengths.

1. Early Far-Infrared Fourier Spectroscopy

Much of the early work carried out under this grant was concerned with the installation of a commercial far-infrared Fourier spectrometer system and subsequent modifications to increase its capabilities. After this work was completed (roughly 18 months into the grant period), the system could provide both transmission and reflection spectra of better than 1 cm^{-1} resolution in the region 10 to 500 cm^{-1}. The system employed a cooled germanium bolometer and required the use of a large digital computer to Fourier transform the raw data.

(NASA-CR-132900) EFFECTS OF SIZE, SHAPE, AND FREQUENCY ON THE ANTIFERROMAGNETIC RESONANCE LINEWIDTH OF MnF Final Technical Report, Nov. 1966 - Jun. 1973 (Brown Univ.) 22 p HC $3.25 CSCL 20L G3/26 N74-17468 Unclas 15679

This system was replaced in 1971 with a state-of-the-art Fourier spectrometer which outperforms the original system by a wide margin (see Section 4); however, some useful information was obtained from the original system. Its operation was checked by observing known antiferromagnetic absorption lines in NiO and MnF_2, and previously unobserved spectra were obtained for $NiCl_2$ and the spinels $NiFe_2O_4$, $MnCr_2O_4$, $MnCr_2S_4$, $CoCr_2S_4$, $FeCr_2S_4$.

These latter compounds have either antiferromagnetic or ferrimagnetic properties, but did not exhibit exchange resonances in the far infrared. If present at all, these lines were masked by numerous vibrational modes. The strength of these absorptions probably precludes the use of these materials in transmission-type submillimeter devices.

2. Antiferromagnetic Resonance in MnF_2 at Millimeter Wavelengths

A detailed experimental and theoretical study of the antiferromagnetic resonance (afmr) linewidth in MnF_2 has been carried out.

Experimental investigations included studies of the shape, size, and frequency dependence of the millimeter wave afmr in MnF_2 at 4.2 K with frequencies ranging from 140 to 305 GHz and magnetic field applied along the symmetry axis. A study of various sample configurations showed that the clearest resonance effects were observed for the case of a very thin sample which filled the cross-section of the waveguide. From both reflection and transmission measurements it was found that the sample thickness should be less than about $\lambda_0/5\varepsilon^{1/2}$ in order that propagation effects be minimized.

Expereimental measurements of transmission through slabs of MnF_2 show that the results do not depend on whether the magnetic field (applied along the symmetry axis) is parallel on perpendicular to the propagation direction. Except at frequencies very far removed (50%) from the zero-field resonance frequency, the linewidth was found to be independent of frequency.

Theoretical investigations include computerized calculation of the r.f. susceptibilities of MnF_2 based on the usual phenomenological molecular field theory. In addition, solutions were obtained for propagation through a slab of saturated, uniaxial magnetic material of both a plane wave with longitudinal applied magnetic field and for the actual modes in a waveguide with transverse magnetic field. These analyses were then combined with the calculated susceptibilities to yield computer-generated curves of the reflection from and transmission through an MnF_2 single crystal as a function of both frequency and magnetic field.

The results of these calculations, when compared with experimental data, show that the lineshape, linewidth, and amount of absorption can be described accurately, within experimental error, by a molecular field based calculation of the susceptibilities with a single adjustable parameter describing relaxation effects. The waveguide analysis gives much better agreement with experimental results than does the commonly used plane-wave analysis, especially with regard to the amount of absorption.

The combined results of these experimental and theoretical studies lead to the following conclusions. The observed linewidth is describable by combined relaxation and dispersion effects and is not due to chemical or physical imperfections in the sample studied. A further conclusion is that previously reported values of afmr linewidths overestimate the intrinsic or relaxation width by at least a factor of two because of dispersion effects in thick samples. For the same reason previous descriptions of the temperature dependence of the linewidth are probably also in error.

The effect of grain misorientation has also been studied. Such misorientation can cause either multiple resonances or line broadening or both. Further, it has been shown that dispersion effects can lead to very significant errors in linewidth measurements made at or very near (within a few percent of) the zero-field resonance frequency.

The general technique used could also be employed in the analysis of experimental results obtained in studies of other types of materials, e.g., ferrites and paramagnets.

These results are further described in three publications which are appended to this report.

3. Numerical Solution of the Equations of Motion of a General Two-Sublattice Antiferromagnet

A general method has been developed for obtaining the solutions to the two-sublattice antiferromagnet equations of motion with arbitrary anisotropy and applied magnetic field. The equilibrium positions of the sublattice magnetizations were found by minimizing the free energy of the system. The equations of motion were then linearized about these equilibrium

positions and were solved for resonant frequencies and natural modes. From these the susceptibility tensor for a single crystal was found. This tensor was then averaged over all applied field directions for a material with easy plane anisotropy, yielding the susceptibility tensor for an easy plane material in powdered or polycrystalline form. Such a material was shown to be highly anisotropic but very nearly reciprocal. The cubic anisotropy case was also examined, and the results obtained were compared with existing theoretical and experimental results of other investigators. The computer calculations agree well with the existing data and reveal more information about the resonant modes; i.e. linear or elliptical polarization of the mode, its orientation in space, and its dependence on the parameters descibing the energy.

4. Antiferromagnetic Resonance in NiO Powder

Antiferromagnetic resonance was observed in NiO single crystals by several investigators in the early 1960's; e.g. Kondoh (1960) and Sievers and Tinkham (1963). A number of other investigators have reported on the difficulty of obtaining NiO crystals of high purity and low defect concentration. It therefore seemed advisable to attempt to observe the antiferromagnetic resonance in powdered NiO which is commercially available in high purity. This was done during the early part of this grant period using the Fourier spectrometer described in Section 1, but the attempt was unsuccessful. This study was reopened in late 1971 after our laboratory

obtained (from funds other than those provided by this grant) a Digilab FTS-14 Fourier spectrometer. This state-of-the-art instrument includes a minicomputer which Fourier transforms the raw data immediately after they are obtained and controls the collection and display of data and spectra. Using the maximum instrument resolution of 0.4 cm^{-1} , the resonance line was observed quite clearly in powdered NiO. Subsequently, the temperature dependence of the location of the resonance line was studied. Results obtained agreed well with earlier single crystal data, and the temperature range over which resonance was observed was extended from 430°K to 470°K using Fourier techniques. This range was further extended up to very near the Neèl temperature of 523°K using coherent millimeter wave energy and microwave techniques. The millimeter resonance data provided a direct, independent determination of the Neèl temperature which is in agreement with that reported by other researchers who measured specific heat and lattice dilation as functions of temperature.

The powder resonance data can be fitted over the entire range of temperature T from 0°K to 523°K with a Brillouin function for S = 1 and Neèl temperature T_n of 523°K to the 0.6 power. Near the Neèl point, the resonant frequency varies as $(T_n - T)^2$, indicating that the out of plane anisotropy constant varies as $(T_n - T)$ near the Neèl point.

5. Resonance Investigations of Several Indium Thiospinels at Millimeter Wavelengths

Studies of the magnetic susceptibilities of the Thiospinels

MIn_2S_4 (= Mn, Ni, Fe, Co) and $MnInCrS_4$ have demonstrated the presence of antiferromagnetic interactions in these compounds. It was therefore felt that magnetic resonance studies might yield useful information about these materials. All of them have been so studied in powdered form with frequencies ranging from 8 to 70 GHz and magnetic field intensities ranging from zero field to about 25 KOe. A variety of microwave spectrometers have been employed - some with cavities, some without.

The existing susceptibility data for $MnInCrS_4$ show a fairly well defined peak at 13°K, indicating a transition to the antiferromagnetic state. The susceptibility data for the other materials are inconclusive ir that very few points were taken at low temperatures and the applied field may have been too high to allow parallel susceptibilities to be observed. The resonance data indicate the following: (a) $MnIn_2S_4$ and $MnInCrS_4$ are strongly paramagnetic with g factors very close to 2 which are with experimental error, temperature independent from room temperature to below 77°K; (b) the resonance field decreases smoothly as temperature is lowered below about 40°K and 20°K for $MnInCrS_4$ and $MnIn_2S_4$, respectively, indicating the presence of magnetic phase transitions; (c) the dependence of resonant frequency on applied field intensity for both of these materials is nearly the same as that for an easy plane antiferromagnet; (d) $MnIn_2S_4$ exhibits a zero field resonance at 10GHz when frequency is swept. There is strong evidence that $MnInCrS_4$ exhibits a zero field resonance near 15GHz, and experiments underway at present will locate this frequency more accurately if it is indeed observed as frequency is swept; (e) MIn_2S_4 (M = Ni, Fe, Co) have exhibited no

resonance whatsoever - even when a high sensitivity EPR spectrometer was employed.

Publications describing the work of this and the previous section are in preparation. Preprints will be forwarded as soon as they are available and are intended to be appended to this report.

Three students have received Ph.D. degress under this program, and two others have received Sc.M. degrees and will shortly be receiving Ph.D. degrees. A list of publications arising from this program follows. These are or are intended to be appended to this report.

1. O'Brien, Kevin C., "Effects of Size, Shape, and Frequency of the Antiferromagnetic Resonance Linewidth in MnF_2," J. Appl. Phys. 41,3713 (1970).

2. O'Brien, Kevin C., "Microwave Properties of Slabs of Uniformly Magnetized Material Filling the Cross Section of a Rectangular Waveguide Operating in TE_{no} Modes," IEEE Trans. MTT-18, 377 (1970).

3. O'Brien, Kevin C., "Microwave Properties of a Rectangular Waveguide Semi-Infinitely Filled with Magnetic Material," IEEE Trans. MTT, MTT-18,400 (1970).

4. Chen, C. H., DeMeo, E. A., Wold, A., Heller, G. S., "Antiferromagnetic Resonance in Powdered NiO," to be published.

5. Hsu, C. I., DeMeo, E. A., Wold, A., Heller, G. S., "Magnetic Resonance Investigation of Several Indium Thiospinels," to be published.

JOURNAL OF APPLIED PHYSICS VOLUME 41, NUMBER 9 AUGUST 1970

Effects of Size, Shape, and Frequency on the Antiferromagnetic Resonance Linewidth of MnF_2*

KEVIN C. O'BRIEN†
Physics Department, Brown University, Providence, Rhode Island 02912

(Received 19 November 1969; in final form 12 March 1970)

Experimental measurements of the antiferromagnetic resonance in MnF_2 at 4.2°K have been made as a function of microwave frequency and sample size and shape. Measurement frequencies ranged from 100 to 305 GHz. The experimental data have been analyzed with the aid of a newly derived electrodynamic treatment of the experimental arrangement combined with a molecular field theoretic calculation of the rf permeability tensor for MnF_2. Agreement between experiment and theory is good using only a one-parameter fit. It was found that the linewidth is not strongly frequency dependent in very good samples except at frequencies very near to or very far from the zero-field resonance frequency. The effect of sample size on observed linewidth is very significant. A value of 90 Oe is given for the residual size-independent linewidth. Experimental aspects are emphasized due to the extremely high frequencies employed.

I. INTRODUCTION

Measurements of the antiferromagnetic resonance (AFMR) in MnF_2 by Johnson and Nethercot[1] and in Cr_2O_3 by Foner[2] have shown a large temperature-independent linewidth at low temperatures.

This anomalous behavior led the author to investigate those extrinsic factors which might affect the measured value of the linewidth. AFMR measurements were made on MnF_2 single crystals at 4.2°K as a function of frequency, sample size and shape.

In order to understand more clearly the frequency and size effects which occur, a careful theoretical treatment of the experimental situation was carried out. The molecular field approximation[3,4] was used to obtain the rf permeability tensor for a uniaxial AFM at 0°K. An exact solution was then obtained for the propagation of TE_{x0} mode microwaves in a rectangular waveguide through a slab of transversely magnetized, magnetically gyrotropic material which completely fills the waveguide cross section. The combination of the computed rf susceptibilities with this exact electrodynamic treatment enables one to carefully analyze experimental data.[5]

AFMR measurements were made on a variety of samples of MnF_2 at frequencies ranging from 100 to 305 GHz at 4.2°K.

II. EXPERIMENTAL CONSIDERATIONS

A. Samples

Manganese difluoride was chosen as the material to be studied because it comes very close to having the ideal two-sublattice uniaxial AFM array of spins. MnF_2 also offers the advantages of being readily available in the form of high-purity good-quality single crystals. Furthermore, its Néel temperature (67°K) is sufficiently high that at liquid-helium temperature (4.2°K) its magnetic properties are close to those at absolute zero. Crystals were grown and oriented by Semi-elements,

B. Spectrometer

A millimeter wave spectrometer was designed and constructed. Due to the fact that AFM's have a high spin density, AFMR absorption is sufficiently large that a microwave cavity need not be used.[7] The spectrometer (diagrammed in Fig. 1) was designed for both transmission and reflection measurements at frequencies ranging from 50 GHz to the highest frequency at which adequate microwave power was available (305 GHz).

Several klystrons were used. Their output frequencies ranged from 50 to 102 GHz with typically 30-mW cw power. The klystron reflector voltages were modulated at 1–4 kHz. Oversized waveguide (RG98) was used wherever possible to reduce transmission losses.[8] A 60-kOe 1-in.-bore Linde superconducting solenoid produced the required dc magnetic fields.

C. Harmonic Generator

The capability of performing measurements above 100 GHz depends critically on the harmonic generator. The harmonic generator used in these experiments was designed and built by Rodgers.[9] It is of the cross-guide type, employing a tungsten cat's whisker to semiconductor junction as the nonlinear element. The condition of the whisker point and crystal surface are critical for good operation. Several types of crystals were tried. Best operation was obtained with an n-type silicon crystal with a high-resistivity epitaxial layer and a bonded nickel contact backing. The operation of such a point-contact diode depends critically on the pressure of the junction contact. For best performance, such a junction, when used as a harmonic generator, requires a somewhat higher contact pressure than when it is used as a detector.

D. Detector

Several types of detectors were tried at the highest frequencies where the signal levels were very low. These included fixed-contact crystal diodes, hot-wire

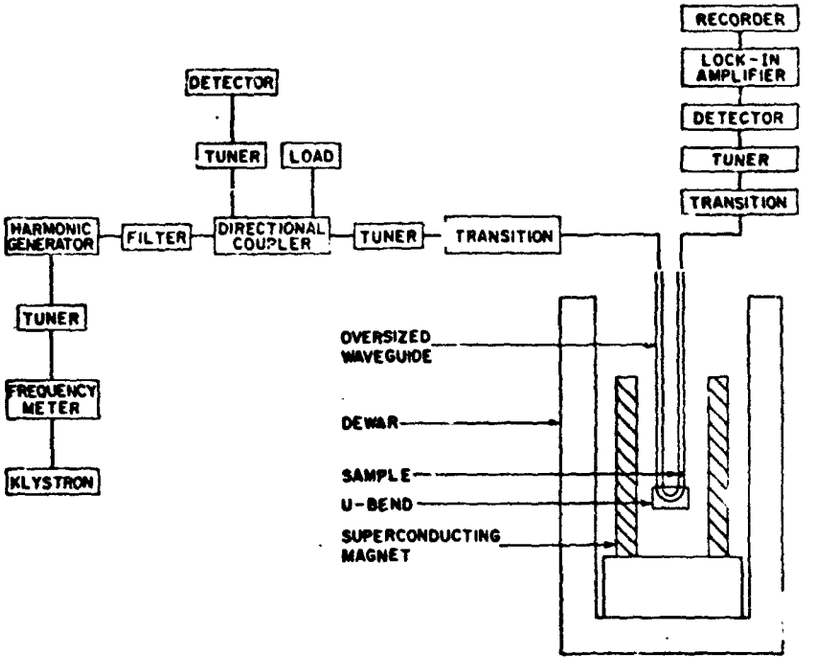

FIG. 1. Schematic diagram of experimental apparatus.

bolometers, a germanium bolometer, a Golay cell, and a "run-in" crystal detector[10] similar in design and method of operation to the harmonic generator. In overall signal to noise the run-in point-contact diode proved best at the highest frequencies. Due to low-frequency (<1 kHz) klystron and harmonic generator noise, the germanium bolometer and Golay cell, although they are intrinsically very sensitive, were not as effective as the run-in detector because they require low (20 Hz) modulation.

It should be pointed out that the cat's whisker–silicon diode, with proper contact, showed no degradation in sensitivity with increasing frequency, even above 300 GHz. Indeed, similar diodes have been used successfully at 10.6 μ.[11] Fixed contact, commercially made detectors do show a clear drop in sensitivity with increasing frequency.

Estimated power levels at the detector end of the spectrometer were 10^{-4} W or less. The minimum detectable power of the run-in detector was 10^{-10}–10^{-11} W. Typical output of the detector was 2μV with 300-nV noise voltage in a 1-Hz bandwidth. Figure 2 shows a typical good experimental trace of transmission through a 0.0025-in. slab filling the waveguide cross section.

E. Experimental Errors

The experimental error in these measurements was $\pm 15\%$ on both the width and amount of absorption. These errors resulted primarily from internal reflection phenomena in the waveguide apparatus, from the low signal-to-noise ratio, from uncertainty in the sample thickness and from the difficulty of fitting the sample exactly into the waveguide cross section.

III. RESULTS

A. Experimental Results

The AFMR in MnF_2 was measured at frequencies ranging from 100 to 305 GHz at 4.2°K. Various arrangements of the sample in the waveguide were tried. Best experimental results were obtained for very thin plates which filled the cross section of the waveguide (Fig. 2). Other sample configurations give results which are very difficult to interpret. Samples much thicker than 0.002 in. showed strong dispersion effects and often gave severe reflection phenomena in association with the

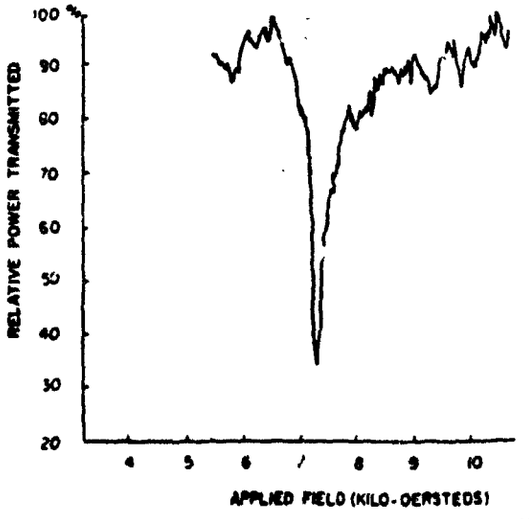

FIG. 2. Typical, good experimental trace. Frequency is 250 GHz. Thickness is 0.0025 in.

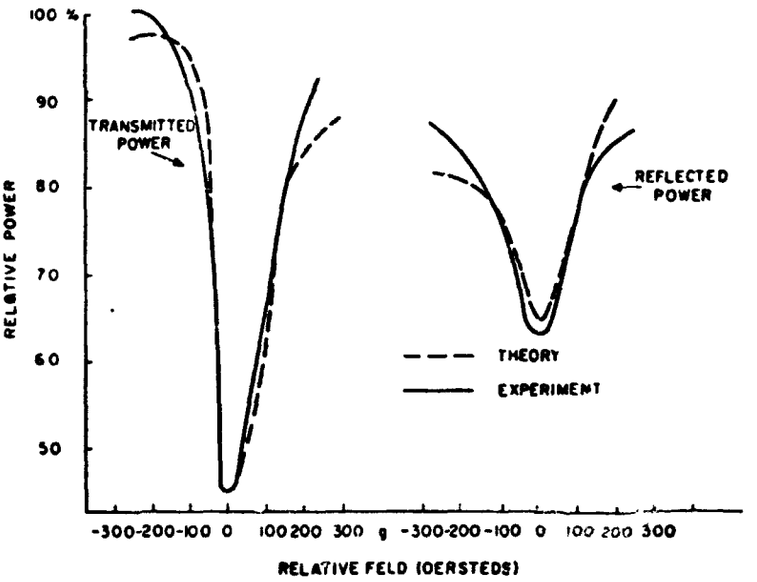

FIG. 3. Comparison of reflected and transmitted powers at 220 GHz. Note that transmitted line is wider on the high-field side, reflected line on the low-field side. Thickness is 0.0025 in.

waveguide components leading to standing waves. Due to the fragility and deliquescence of MnF_2 crystals, preparation of samples less than 0.002-in. thick is very difficult. Typical measured transmission linewidths[12] were 120–166 Oe for a 0.0025-in. sample (see below). In the best crystals the linewidths were nearly independent of frequency except at very high fields and at frequencies very near the zero-field resonance frequency. The shape of the resonance was clearly asymmetric, as reported by Johnson and Nethercot.[1]

The energy reflected from the sample exhibits resonant behavior (Fig. 3). The reflected line is asymmetric also, but has the opposite asymmetry from the transmitted line. The minima of the reflected and transmitted lines may occur at slightly different values of the applied field. Measurements at high applied magnetic fields showed increased linewidth. This effect is almost certainly due to small amounts of grain misorientation in the crystals.[6] It suggests that high magnetic field resonance measurements should be made only on extremely good crystals. At frequencies very near the zero-field resonance frequency, however, very strong asymmetries were observed (Fig. 4). This effect is predicted by the theory and is due to a combination of dispersive effects and the overlap of the resonance on the other branch. A resonance measurement taken exactly at zero field will be substantially broadened compared to one taken at some significant applied field, although this field may be small compared to the critical field.

Experimental data taken in the course of this experiment show that the resonance linewidth is a strong function of the sample thickness. This effect was very difficult to measure quantitatively because of the difficulties in sample preparation and because of the fact that complex propagation effects were observed in measurements on thicker samples. The thick samples, in conjunction with waveguide component discontinuities, produced standing waves in the spectrometer.

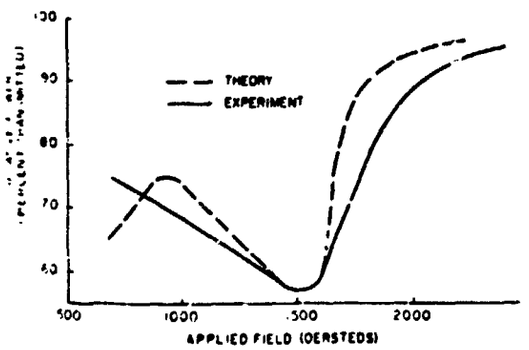

FIG. 4. Anomalous broadening observed at frequency slightly above zero-field resonance frequency. Thickness is 0.0025 in.

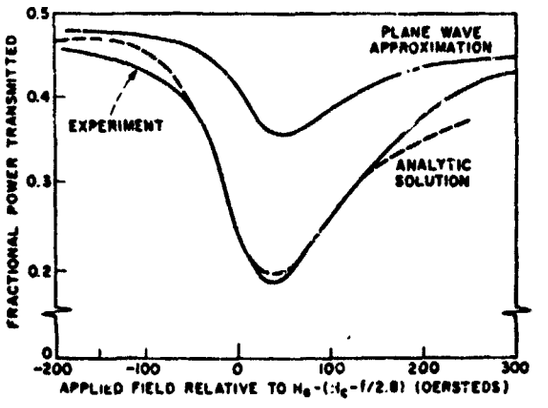

FIG. 5. Comparison of experimental data with plane wave approximation and exact waveguide solution. Frequency is 250 GHz. Thickness is 0.0025 in.

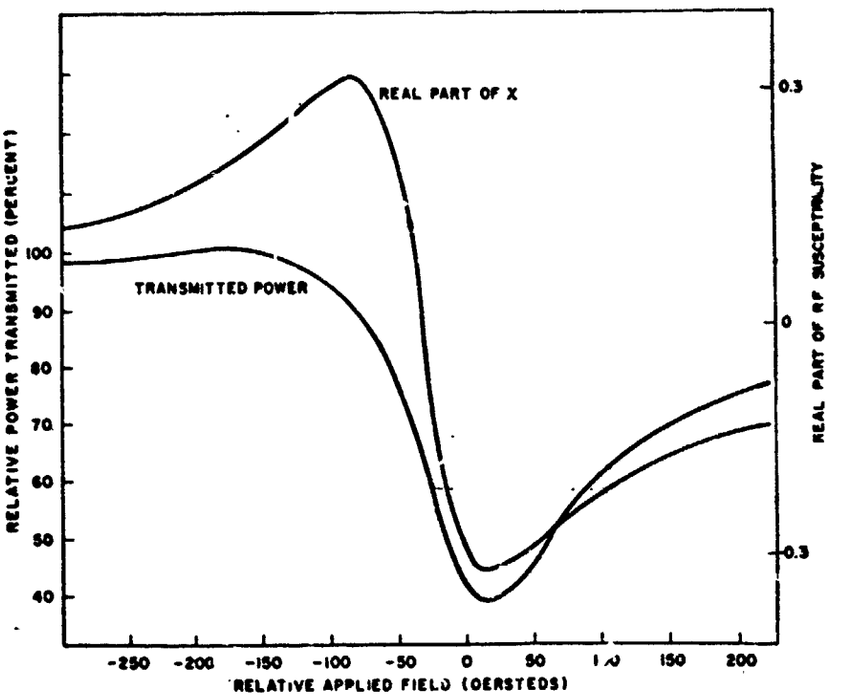

FIG. 6. Shows relation [illegible] real part of rf susce[illegible] shape of transmitted [illegible] Frequency = 250 GHz. Th[illegible] is 0.0025 in.

It was clear nonetheless that thick samples (0.005–0.010 in.) showed linewidths a factor of two or more greater than those seen in 0.002-in. samples.

B. Theoretical Results

In order to verify the usefulness of the exact electrodynamic waveguide solution described above, a similar calculation was performed in a plane wave approximation.[18] In Fig. 5 experimental results are compared with theoretical predictions of the plane wave approximation and of the exact waveguide solution. In both cases, the width is an adjustable parameter but the shape and magnitude come directly from the theory. Only one adjustable parameter is used, a parameter describing simple Gilbert damping.[4] The results of the plane wave calculation do not compare well with experimental data quantitatively, even though qualitatively they do give the shape of the resonance fairly well. Although it would not be difficult to adjust the magnitude of the plane wave results so that the fit with experimental data would be better; to do so serves no useful purpose. (If the magnitude were increased, the relaxation width loss parameter would have to be decreased.)

The lack of agreement between experiment and the plane wave calculation might seem surprising since an oversized waveguide was used. The waveguide was, however, not so far oversized that plane waves at normal incidence are a good representation of the actual modes especially inside the magnetic medium.

On the other hand it is clear that the results of the waveguide solution (Fig. 5) fit the experimental data quite well both with respect to shape and magnitude. The experimental curve shown is the average of several runs. The theoretical results clearly reflect both the change in the direction of the asymmetry with branch and the larger asymmetry found near the zero-field resonance.

Figure 5 shows a measured transmission width of 150 Oe. On the low-field (narrow) side of the line, the half-width is approximately 50 [illegible] the high-field (wide) side of the line the half width is approximately 100 Oe. Figure 6 indicates the relation between the real or dispersive part of the susceptibility and the high-field broadening of the line. Calculations show that an increase in sample thickness affects the high-field (wide) side much more than the low-field side, thus indicating that this thickness broadening is primarily dispersive in nature and is not due to a simple saturation effect.

The agreement between theory and experiment is not as good on the wings of the resonance as it is near the center. This is to be expected since dispersion is most important on the wings and would be very sensitive to any nonparallelism or irregularities in the sample shape.

C. Effect of Sample Thickness on Linewidth

As described in above, thick samples showed substantially greater linewidths than did thin samples. Theoretical calculations (shown in Fig. 7) indicate that the observed linewidth depends very strongly on the sample thickness. Furthermore this broadening was seen to be primarily dispersive in origin rather than caused by a saturation effect. Earlier measurements on MnF_2 were made on samples whose thickness was near to $\lambda_0/4(\epsilon)^{1/2}$ (λ_0 is the free-space wavelength and ϵ is the dielectric constant.) Those experiments gave linewidths

near to 300 Oe. The present measurements on samples roughly $\lambda_0/8(\epsilon)^{1/2}$ gave linewidths of about 150 Oe. Extrapolation of these data by means of current theoretical treatment leads to the conclusion that extremely thin samples, say $\lambda_0/20(\epsilon)^{1/2}$ thick or less would show a width of about 90 Oe. This value of 90 Oe is consistent with the theoretical-to-experimental fit shown in Fig. 5. It is clear therefore that AFMR linewidth measurements made on thick samples will yield data which may be highly inaccurate unless this size effect is taken into account.

Even this 90-Oe width is substantially larger than that predicted by spin wave relaxation processes ($\sim$1 Oe) [14] and so might be expected to be due to some inhomogeneities. On the other hand, although a simple molecular field theoretic relaxation process was used the experimental data fits the theory well under a variety of circumstances. The residual width did not vary significantly from sample to sample. I would thus hesitate to conclude that the residual width is not due to relaxation processes without a careful study of the temperature dependence of the width. Reports of the temperature dependence of the linewidth of both MnF_2[1] and Cr_2O_3[2] show that the linewidth is independent of temperature at low temperatures. This is not to be expected on theoretical grounds[14] since the thermal disordering of the magnetic system would presumably increase the variation in effective fields through the sample. In light of the size effect discussed above, it is likely that what was observed in those experiments was a dispersion width which was independent of temperature. Only when the intrinsic width increased with temperature to the point where it exceeded the dispersion width was a temperature variation observed.

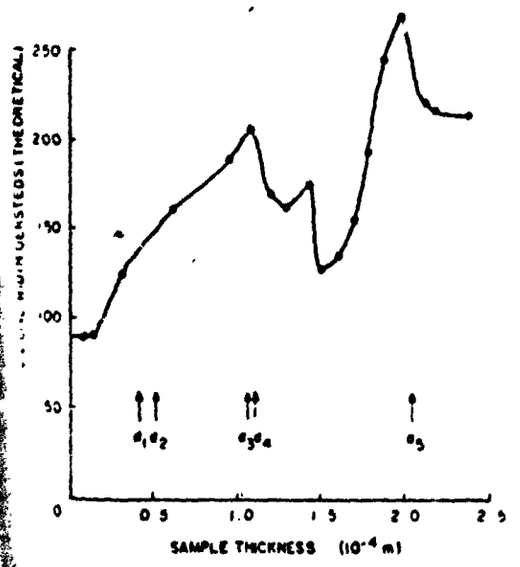

FIG. 7. Theoretical calculation of transmission linewidth vs sample thickness at 270 GHz. $d_1=\lambda_0/10\epsilon^{1/2}$, d_2 = minimum thickness used in this work (0.0025 in.), $d_3=\lambda_0/4\epsilon^{1/2}$, d_4 = thickness used by Johnson and Nethercot, $d_5=\lambda_0/2\epsilon^{1/2}$.

Accurate experimental values of the temperature dependence of the linewidth in these materials must await experimental measurements on very thin samples. These measurements must be combined with a theoretical analysis based on both temperature dependent values of the rf susceptibility and an accurate electrodynamic treatment such as used here. Such measurements are now being planned.

IV. CONCLUSIONS

By combining measurements of the effects of frequency, sample size and shape for the AFMR linewidth of MnF_2 with a careful, complete calculation of the microwave propagation problem it has been found that resonance measurements made on samples thicker than $\lambda/10(\epsilon)^{1/2}$ will show strong dispersive broadening. This broadening can be accounted for by a careful calculation. A residual width of 90–130 Oe is found. This width is probably not due to crystalline imperfections since it has been observed in several samples. This residual width is nearly independent of frequency. Theoretical explanations of the source of this width must await further investigations especially of its temperature dependence.

ACKNOWLEDGMENTS

The author extends his gratitude to Professor Gerald S. Heller who directed this work and to Professor Donald M. Bolle and Mr. Ching-hi Hsu who provided a great deal of assistance during the course of this work.

* This work was supported in part under NASA Grant NGR 40-002-042.

† Present address: Bell Telephone Laboratories, Whippany Road, Whippany, N.J. 07981.

[1] F. M. Johnson and A. H. Nethercot, Phys. Rev. 114, 705 (1959).

[2] S. Foner, Phys. Rev. 130, 183 (1963).

[3] F. Keffer and C. Kittel, Phys. Rev. 85, 329 (1952).

[4] G. S. Heller, J. J. Stickler, and R. B. Thaxter, J. Appl. Phys. 32, 307S (1961).

[5] Most measurements were actually made with longitudinal magnetization. Although not theoretically predicted, experimental results show that AFMR measurements on thin MnF_2 slabs filling the waveguide cross section do not depend significantly on whether the applied field is transverse or longitudinal to the propagation direction. This mathematical analysis will be described in a forthcoming paper in IEEE Trans. Microwave Theory Tech. 18, 7 (1970).

[6] Address: Saxonburg Blvd., Saxonburg, Pa. Small errors in overall crystal orientation have little effect. Extensive grain misalignment will, however, produce spurious effects such as the double resonances observed by Johnson and Nethercot (Ref. 1).

[7] AFMR is, however, relatively weak (gram for gram) compared to ferrimagnetic resonance giving perhaps five to ten times less absorption.

[8] Fundamental mode waveguide at 300 GHz has an attenuation of at least 1 dB/in.

[9] Address: Box # 50, Cherry Hill Rd., Baltimore, Md. 21013.

[10] It is called a "run-in" detector because the whisker is run through the waveguide by means of a differential screw for adjustment of the contact pressure.

[11] L. L. Hocker, D. R. Sokoloff, V. Danciu, A. Szoke and A. A. Javan, Appl. Phys. Lett 12, 401 (1968).

[12] Full width between points where transmitted power falls to one-half its nonresonant value.

[13] See, for example: A. G. Gurevich, *Ferrites at Microwave Frequencies*. (Consultants Bureau, New York, 1963).

[14] A. B. Harris, J. Appl. Phys. 37, 1128 (1966).

[8] L. D. Smullin and H. A. Haus, Eds., *Noise in Electron Devices*. Cambridge, Mass.: M.I.T. Press, 1959, p. 214.
[9] A. van der Ziel, *Noise*. New York: Prentice-Hall, 1954, pp. 65–69.
[10] Test no. 7824, General Electric Company, Nela Park, Cleveland, Ohio.
[11] W. E. Forsythe, *Smithsonian Physical Tables*, 9th rev. ed. Washington, D.C.: Smithsonian Institution, 1964, Table 85.
[12] R. E. Guentzler, "Additional data on the monode noise generator," *QST*, vol. 53, pp. 50–51, August 1969.
[13] IRE Subcommittee 7.9 on Noise, H. A. Haus, Chairman, "Representation of noise in linear twoports," *Proc. IRE*, vol. 48, pp. 69–74, January 1960.
[14] R. D. Cutkosky, "A varactor null detector for audio frequency capacitance bridges," *IEEE Trans. Instrumentation and Measurement*, vol. IM-17, pp. 232–238, December 1968.
[15] D. M. Speros and P. R. Bucciili, "Method and apparatus for measuring the starting characteristics of gas filled discharge lamps," U. S. Patent 3 249 859, May 3, 1966.
[16] E. Maxwell and B. J. Leon, "Absolute measurement of receiver noise figures at UHF," *IRE Trans. Microwave Theory and Techniques*, vol. MTT-4, pp. 81–85, April 1956.
[17] I. Chinnock, "A portable direct-reading microwave noise generator," *Proc IRE*, vol. 40, pp. 160–164, February 1952.
[18] C. E. Beck, General Electric Company, Nela Park, Cleveland, Ohio, private communication.

Correspondence

Microwave Properties of a Rectangular Waveguide Semi-Infinitely Filled with Magnetic Material

***Abstract*—An infinite, lossless, rectangular waveguide semi-infinitely filled with a transversely magnetized magnetic material is discussed. With the limitation that only TE_{n0} modes are incident, an analytic solution for the transmitted and reflected energies is presented. Numerical computations near resonance are presented both for a ferrite and an easy-axis antiferromagnet.**

Many microwave measurements and devices using magnetic materials require an analysis of wave propagation in partially filled waveguides. (General treatments and references to this whole area are presented in [1] and [2]). Many authors have treated such problems. Of special importance is the work of Seavey and Tannenwald [3], Epstein [4], and Rosenbaum [5]. Only a limited class of problems in this area can be treated analytically [1]. This correspondence presents such an analytic treatment for a rectangular waveguide semi-infinitely filled with transversely magnetized material. Although semi-infinite filled waveguides have little practical application, it may be an acceptable approximation to some physical cases and the techniques used here can be extended to waveguides filled over a finite length. The problem of propagation in a semi-infinitely filled coaxial line has been treated by Brodwin and Miller [6] using the same approach.

In this correspondence, the TE_{n0} modes in empty and filled waveguide are matched at a plane boundary. A general matrix equation is derived. An approximate numerical inversion of this matrix equation is performed for the cases of a simple ferromagnet and for a uniaxial antiferromagnet in the vicinity of the resonance.

Specifically we shall consider the problem of an infinite, lossless, rectangular waveguide operating only in TE_{n0} modes which is semi-infinitely filled with magnetic material. The material is taken to be uniformly magnetized by a dc magnetic field applied normal to the broad wall of the waveguide (y direction). The boundary (at $z=0$) between the empty and filled regions is taken to be a plane normal to the propagation (z) direction. Even if only one TE_{n0} mode is incident, we must assume that all TE_{n0} modes are generated at the interface if we are to satisfy the boundary conditions.

The TE_{n0} modes of amplitude A_n in an empty waveguide of wide dimension a and narrow dimension $a/2$ can be written, assuming $\exp(j\omega t)$ time dependence [7]. (The z components do not enter into the solution and are thus not written down.)

$$\begin{aligned} e_x^n &= e_z^n = 0 \\ e_y^n &= A_n \sin(nv) \exp(\mp j\beta_n z) \\ h_y^n &= 0 \\ h_z^n &= \mp (\beta_n/\omega\mu_0) A_n \sin(nv) \exp(\mp j\beta_n z) \end{aligned} \tag{1}$$

where

$$\begin{aligned} \beta_n^2 &= \omega^2\mu_0\epsilon_0 - (n\pi/a)^2 \\ v &= \pi x/a. \end{aligned} \tag{2}$$

The response of a magnetic material to RF magnetic fields must be described by a tensor permeability which in the present circumstance is taken to have the Polder form

$$\mu = 1 + \chi = \begin{vmatrix} 1+\chi & -j\kappa & 0 \\ 0 & 1 & 0 \\ j\kappa & 0 & 1+\chi \end{vmatrix}. \tag{3}$$

Using μ in Maxwell's equations one finds for the TE_{n0} modes in a filled waveguide [1]–[3]

$$\begin{aligned} e_x^n &= e_z^n = 0 \\ e_y^n &= A_n \sin(nv) \exp(\mp j\gamma_n z) \\ h_y^n &= 0 \\ h_z^n &= [\mp \zeta\gamma_n A_n \sin(nv) \\ &\quad - \xi A_n n \cos(nv)] \exp(\mp j\gamma_n z) \end{aligned} \tag{4}$$

where

$$\begin{aligned} \gamma_n^2 &= \omega^2\mu_0\epsilon\mu_{eff} - \left(\frac{n\pi}{a}\right)^2 \\ \zeta &= 1/\omega\mu_0\mu_{eff} \\ \xi &= (\pi/a)(\kappa/\mu)\zeta \\ \mu &= 1 + \chi \\ \mu_{eff} &= (\mu^2 - \kappa^2)/\mu. \end{aligned}$$

It is necessary to consider three independent waves, incident, reflected, and transmitted. The incident wave is, of course, known and the transmitted wave is essentially immeasurable so we calculate only the reflected power. Of particular interest is the reflected power as the magnetic material passes through resonance.

The relevant boundary conditions are that the tangential electric and magnetic fields be continuous across the boundary between the empty and filled regions. Thus, at $z=0$

$$e_{inc} + e_{refl} = e_{trans} \tag{5a}$$

$$h_{inc} + h_{refl} = h_{trans}. \tag{5b}$$

We consider the general case of the incident wave being made up of all TE_{n0} modes; the reflected and transmitted waves would contain all TE_{n0} modes even if the incident wave did not. The incident, reflected, and transmitted electric and magnetic fields can be written, with amplitudes I_n, R_n, and T_n, respectively,

$$\begin{aligned} e_y^I &= \sum_r I_r \sin(rv) \exp(-j\beta_r z) \\ h_z^I &= -\sum_r g_r I_r \sin(rv) \exp(-j\beta_r z) \\ e_y^R &= -\sum_p R_p \sin(pv) \exp(+j\beta_p z) \\ h_z^R &= -\sum_p g_p R_p \sin(pv) \exp(+j\beta_p z) \\ e_y^T &= \sum_q T_q \sin(qv) \exp(-j\gamma_q z) \\ h_z^T &= -\sum_q T_q [\zeta\gamma_q \sin(qv) + \xi q \cos(qv)] \\ &\quad \cdot \exp(-j\gamma_q z) \end{aligned} \tag{6}$$

where

$$g_n = \beta_n/\omega\mu_0.$$

Manuscript received May 1, 1969; revised October 13, 1969. This work was performed under NASA Grant NGR-49-002-042.

There is no boundary condition on the h_n's so they do not enter into the equations. If we place (6) into (5a) and (5b) and operate on all equations with

$$(2/\pi)\int_0^\pi dx \sin(nx), \tag{7}$$

we obtain

$$I_n - R_n = T_n \tag{8a}$$

$$-g_n I_n - g_n R_n = -j\gamma_n T_n - \xi \sum M_{nq} T_q \tag{8b}$$

where

$$M_{nq} = (2/\pi)q\int_0^\pi dx \sin(nx)\cos(qx)$$
$$= 0, \quad n = q$$
$$= (2/\pi)[1-(-1)^{n+q}]nq/(n^2-q^2), \quad n \neq q. \tag{9}$$

For the sake of mathematical convenience we eliminate the R_n's from (8a) and (b). Then we have a set of equations to be solved for the T_n's, $n = 1,2,\cdots,N$, where N is to be chosen by a process of trial and error. (See below for significance of choosing different values of N.)

$$2g_n I_n/\xi = \sum_q [M_{nq} + (g_n + j\gamma_n)\delta_{nq}/\xi]T_q. \tag{10}$$

This has the general form of the matrix equation

$$b = (M + D)t \tag{11}$$

where b is the input vector, D is a diagonal matrix, and t is the vector of transmission amplitudes. The antisymmetric matrix M does not converge, rather the element $M_{n,n+1}$ increases without bound as n increases. Nonetheless, in practice inversion of (10) is possible for any desired N. Note that M is singular for N odd so that this case should be avoided since D has complex behavior near resonance.

It is now required to calculate the RF susceptibilities of the magnetic material to be considered. We shall treat two cases: a simple ferromagnetic insulator[1] and an easy-axis antiferromagnet, including loss for each case. The susceptibility calculation for the ferromagnet is straightforward [10]. We employ the Gilbert[2] form of introducing loss into the equations of motion, and find for the element of the permeability tensor

$$\chi = (\chi^+ + \chi^-)/2$$
$$\kappa = (\chi^+ - \chi^-)/2$$
$$\chi^\pm = \frac{\pm M_0}{(\omega/\gamma) \pm (H_0 + j\Delta H/2)} \tag{12}$$

where M_0 is the bulk magnetization and ΔH is the resonance linewidth. The resonant condition is $\omega = \gamma H_0$ where $\gamma = 2.8$ MHz/oe. For an antiferromagnet the susceptibility calculation is somewhat more complicated [11]. We consider the simple case of an easy-axis antiferromagnet with the easy axis aligned with the applied field. Following the technique of Heller *et al.* [12], we find

$$\chi^\pm = \frac{-2K(1+j\Delta H/H_e)[(\omega/\gamma \pm H_0)^2 - H_e^2 + j\Delta H H_e]}{[(\omega/\gamma \pm H_0)^2 - H_e^2]^2 + (\Delta H)^2 H_e^2} \tag{13}$$

where (12) still holds and K is the anisotropy constant. The resonant condition is $\omega = \gamma(H_e \pm H_0)$ where H_e depends on the material to be considered. We shall treat MnF_2 at 0°K where $H_e = 93$ k-oe. Note that there are two branches of the resonance. Thus, for a given applied field, resonance occurs at two frequencies $\omega = \gamma(H_e + H_0)$ (upper branch) and $\omega = \gamma(H_e - H_0)$ (lower branch).

Inserting the appropriate values of χ, κ, and I_n into (10), we can obtain the solution for any desired number of modes. After solving for the T_n's, (8a) easily yields the R_n's. As mentioned before M does not converge, but upon solving (10) for the case $I_n = \delta_{n1}$, that is only a TE_{10} mode incident, we find that virtually all the reflected and transmitted energy is contained in the TE_{10} modes. The energy contained in modes higher than the incident mode is nonzero but of *insignificant* magnitude. The calculation was carried out on a computer for the first four and for the first ten modes. No significant differences were observed for the two cases.

Fig. 1 shows the reflected power for the ferromagnetic case and Fig. 2 for the antiferromagnetic case.

Similar, although more complicated, techniques may be applied to the problem of a finite layer of magnetic material filling the cross section of the waveguide and other similar problems. The results of these analyses will be presented in a later paper [13].

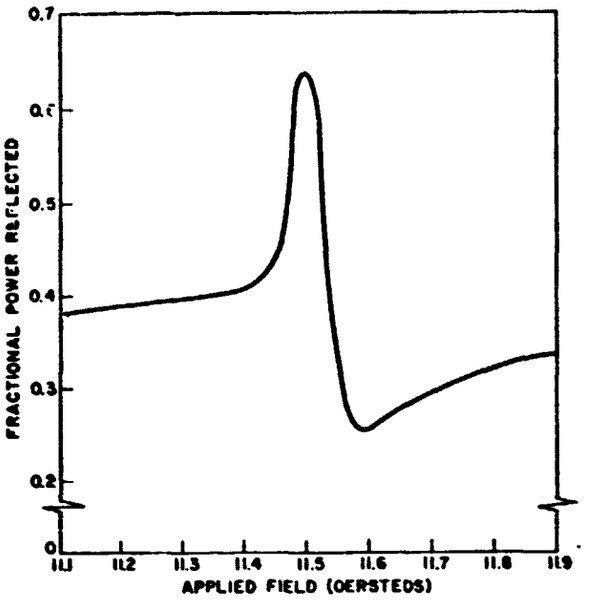

Fig. 1. Fractional power reflected from semi-infinite ferrite in RG96 waveguide. Frequency = 35 GHz; magnetization 100 oe; linewidth = 100 oe; dielectric constant = 10. Computed curve.

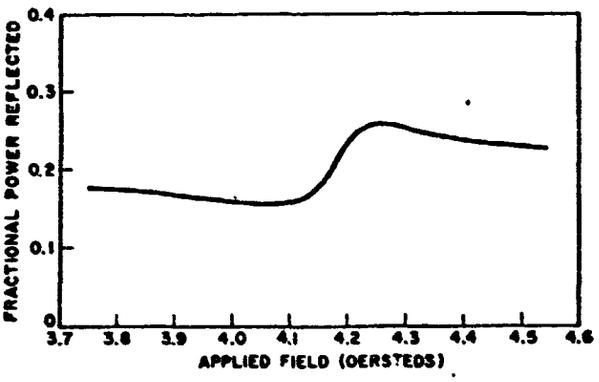

Fig. 2. Fractional power reflected from semi-infinite MnF_2 single crystal in RG98 waveguide. Frequency = 230 GHz; linewidth = 90 oe; dielectric constant = 6.7; temperature = 0°K. The symmetry axis of the crystal is parallel to the applied field. Computed curve.

[1] Anisotropy and demagnetizing effects are not included for reasons of simplicity. Any desired forms of the susceptibility could be used.

[2] The Gilbert form [8] is another, but convenient, form of Landau-Lifshitz damping. See [9] for a good discussion.

ACKNOWLEDGMENT

The author wishes to extend his appreciation to Prof. G. S. Heller and D. M. Bolle for their assistance in this work.

KEVIN C. O'BRIEN[a]
Dept. of Physics
Brown University
Providence, R. I.

REFERENCES

[1] A. G. Gurevich, *Ferrites at Microwave Frequencies*. Consultants Bureau, New York: 1963. Especially chs. VII–IX.
[2] B. Lax and K. J. Button, *Microwave Ferrites and Ferrimagnetics*. New York: McGraw-Hill, 1962. Especially chs. 7 and 9.
[3] M. H. Seavey and P. E. Tannenwald "Electromagnetic propagation effects in ferromagnetic resonance," M.I.T. Lincoln Laboratory, Lexington, Mass., Tech. Rept. 143, 1957.
[4] P. S. Epstein, *Usp. Fiz. Nauk*, vol. 65, p. 238, 1958.
[5] F. J. Rosenbaum, "Electromagnetic wave propagation in lossy ferrites," *IEEE Trans. Microwave Theory and Techniques*, vol. MTT-12, pp. 517–528, September 1964.
[6] M. E. Brodwin and D. A. Miller, "Propagation of the quasi-TEM mode in ferrite-filled coaxial line," *IEEE Trans. Microwave Theory and Techniques*, vol. MTT-12, pp. 496–503, September 1964.
[7] R. E. Collin, *Foundations of Microwave Engineering*. New York: McGraw-Hill, 1960, p. 102.
[8] T. A. Gilbert, Armour Research Institute, unpublished report.
[9] C. W. Haas and H. B. Callen, in *Magnetism*, vol. I, G. T. Rado and H. Suhl, Eds. New York: Academic Press, 1963, ch. 10.
[10] A. H. Morrish, *The Physical Principles of Magnetism*. New York: Wiley, 1965 p. 542.
[11] F. Keffer and C. Kittel, "Theory of antiferromagnetic resonance," *Phys. Rev.*, vol. 85, p. 329, 1952.
[12] G. S. Heller *et al.*, "Antiferromagnetic materials for millimeter and submillimeter devices," *J. Appl. Phys.*, vol. 32, Suppl. 3, p. 307S, 1961.
[13] K. C. O'Brien, "Microwave properties of slabs of uniformly magnetized material filling the cross section of a rectangular waveguide operating in TE_{m0} modes," this issue, pp. 377–382.

[a] Presently with Bell Telephone Labs., Inc., Whippany, N. J.

Design Tables for a Class of Optimum Microwave Bandstop Filters

***Abstract*—Element value tables for optimum microwave bandstop filters consisting of quarter-wave spaced shunt open-circuited stubs are given. Both the stubs and the connecting unit elements contribute to the attenuation response. The tables give element values for 0.01 dB, 0.10 dB, and 0.25 dB ripple Chebyshev designs with up to twenty-three elements, and for bandwidths between 30 percent and 150 percent.**

An important class of microwave bandstop filters (often used as pseudo low-pass filters) that can be realized using stripline structures is shown in Fig. 1. Several authors [1]–[4] have given exact design procedures for filters of this form. These design procedures start with the transmission line equivalent of the low-pass filter of m_{th} order (where m is the number of L-C stub-type elements) in tandem with $m-1$ unit elements of the same characteristic impedance as the load, and then utilize Kuroda's identities to obtain the desired network of Fig. 1. With the above design method the unit elements are redundant, and their filtering properties are not utilized.

Several authors [5], [6] have given the procedure for constructing optimum insertion loss functions which can be realized by a network consisting of unit elements and stubs. Horton and Wenzel [5], [7] have compared the utility of unit elements with those of stubs in the case of doubly terminated filter networks, and have found that for bandstop filters with wide stopbands, unit elements are nearly as effective as stubs. By incorporating the unit elements in the design, significantly steeper attenuation characteristics can be obtained for the same number of stubs than is possible for filters designed with redundant unit elements. Also, a specified filter characteristic can be obtained in a more compact configuration if the network is designed by the optimum method.

To illustrate the advantages of the optimum design approach, the attenuation characteristic of an optimum 0.1-dB ripple five-stub bandstop filter of 120 percent bandwidth is compared in Fig. 2 with a five-stub redundant unit-element design. If it is required that the 120 percent bandwidth 0.1-dB ripple bandstop filter be designed with a constraint that the 30-dB bandwidth be greater than 100 percent, then a filter with but five stubs (and four unit elements) is sufficient if the optimum design is used. If the redundant method is used, then at least eight stubs (and seven unit elements) would be required, and the stripline filter would be almost double in length.

In this correspondence tables of normalized characteristic admittance values (C and Y) are presented [8] for doubly terminated Chebyshev filters of the form shown in Fig. 1. The tables were obtained by synthesis starting from the low-pass gain functions [5]

$$|t|^2 = \frac{1}{1+\epsilon^2\left\{T_m\left(\frac{S}{S_c}\right)T_{m-1}\left(\frac{S\sqrt{1-S_c^2}}{S_c\sqrt{1-S^2}}\right) - U_m\left(\frac{S}{S_c}\right)U_{m-1}\left(\frac{S\sqrt{1-S_c^2}}{S_c\sqrt{1-S^2}}\right)\right\}^2}, \quad (1)$$

where

$S = j\Omega = j\tan(\pi f/2f_0)$, the Richards' transform variable
f is real frequency
f_0 is the frequency for which the lines are a quarter wave-length long
$S_c = j\Omega_c = j\tan(\pi f_c/2f_0)$ is the prototype cutoff frequency
$\epsilon = (10^{r/10}-1)^{1/2}$ is the ripple factor
r = passband ripple value in dB
m is the number of stubs
T_m and U_m are the Chebyshev polynomials of the first and second kind, respectively.

Although the synthesis can be accomplished using conventional techniques in the S variable of (1), the synthesis was actually performed in the transformed variable $W = \sqrt{1-S_c^2}/S^2$ described in Horton and Wenzel [5] using techniques similar to those presented in Bingham [9]. The transformed variable was used to alleviate a computer numerical accuracy problem for filters with many sections.

In computing element values, the S_c parameter of (1) was chosen to give the desired percentage bandwidth by the relation

$$S_c = j\Omega_c = j\tan\{(2-X)\pi/4\}$$

where

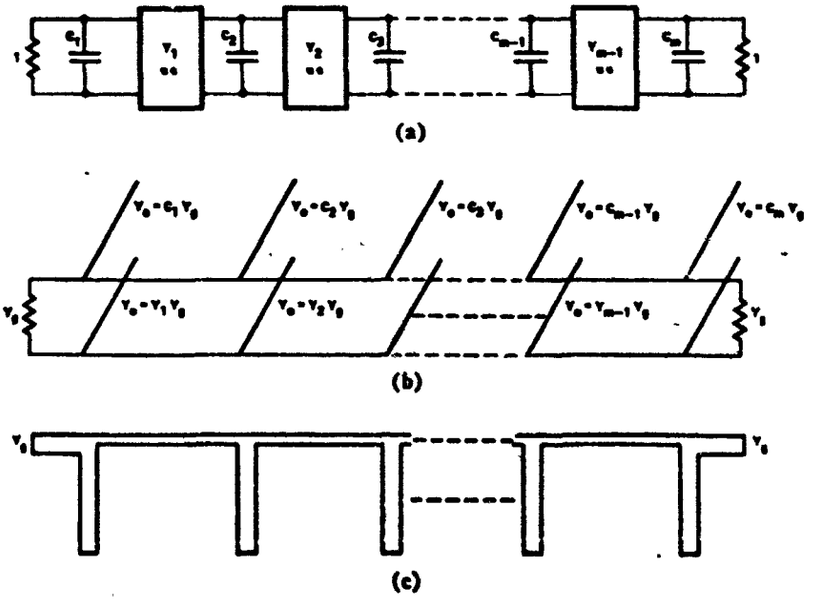

Fig. 1. Microwave bandstop filter networks. (a) "S-plane" prototype network. (b) Transmission line prototype network. (c) Stripline physical realization.

Manuscript received September 17, 1969, revised January 23, 1970.

Microwave Properties of Slabs of Uniformly Magnetized Material Filling the Cross Section of a Rectangular Waveguide Operating in TE_{NO} Modes

KEVIN C. O'BRIEN, MEMBER, IEEE

Abstract—The microwave properties of a slab of uniformly magnetized material filling the cross section of an infinite, lossless rectangular waveguide operating only in TE_{NO} modes are discussed analytically. The material is assumed to have a scalar permittivity and a permeability describable by a tensor of the Polder form. A dc magnetic field is applied normal to the broad wall of the waveguide. Two cases are treated in detail. 1) The slab is placed against a metal shorting wall. 2) The slab is placed with empty waveguide on each side. A general analytical solution is obtained for both cases. Numerical values are computed for MnF_2, an easy-axis antiferromagnet. The computed values for the second are compared with values calculated on the basis of a plane-wave approximation and with experimental data. Applications of the technique to experimental measurements are described.

I. Introduction

EXPERIMENTAL measurements of the microwave properties of magnetic materials have usually been analyzed by means of some electrodynamic approximation to the actual experimental situation. For example, the waveguide modes may be approximated by plane waves or the effect of the sample may be treated as a perturbation on the usual waveguide modes [1], [2]. Although such approximations are generally adequate to describe the qualitative aspects of the experimental data, good quantitative agreement between theory and experiment is difficult to obtain. There are, however, some experimentally practical situations which can be analyzed exactly [3]–[6]. Two such situations will be discussed here.

Consider first the general problem of a slab of material filling the cross section of a rectangular waveguide as diagramed in Fig. 1(a). The following conditions are assumed: the waveguide is lossless and has a rectangular cross section with width twice its height; the slab is plane-parallel and completely fills the waveguide cross section; the material has scalar permittivity and tensor permeability of the Polder [3] form; the material is uniformly magnetized by a dc magnetic field applied normal to the broad wall of the waveguide; all waves consist only of TE_{no} modes, that is, the RF electric fields have components only along the direction of the applied field (the y direction) and the RF magnetic fields have no y components.

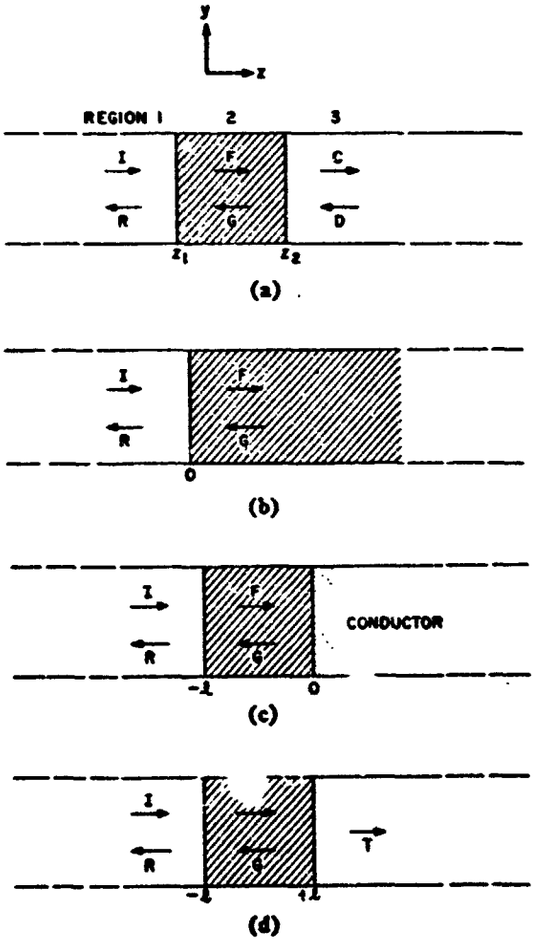

Fig. 1. (a) General problem. (b) Semi-infinite medium. (c) Slab in shorted waveguide. (d) Slab in open waveguide.

The problem of magnetic material in waveguides has a long and complex history. No attempt will be made here to review that history since it is well covered in [1] and [2]. References [3]–[16] cover some of the high-

Manuscript received October 8, 1969; revised January 12, 1970. This work was supported by NASA Grant NGR 40-002-042.

The author was with the Physics Department, Brown University, Providence, R. I. He is now with Bell Telephone Laboratories, Whippany, N. J. 07981.

lights. As early as 1953 [4], [5], the waveguide modes in transversely magnetized media were known. The mathematical complexities associated with the air-magnetic material interface have hindered progress [15]. As will be seen, the approach used here is somewhat different, although straightforward, from that used by many previous authors. (See [6] however.) It is hoped that this technique can be extended to other related problems.

It would be worthwhile to consider briefly the problem of the semi-infinitely filled waveguide [17] [Fig. 1(b)]. The incident wave called I breaks up into waves R and F, the reflected and transmitted waves. The boundary conditions are the usual ones—the tangential electric and magnetic fields are continuous across the boundary. In order to satisfy these boundary conditions (because of the form of the modes in the magnetic material) even if the incident wave is purely TE_{10}, waves R and F must be assumed to consist of all TE_{NO} modes.[1] Thus, R and F must be represented as sums of an infinite number of TE_{NO} modes of the form appropriate to the medium in question. This factor makes the solution of this problem enormously more difficult than the equivalent problem for scalar media. It becomes clear, however, once the calculations are complete, that although the higher order modes are mathematically significant (that is, there is no mathematical convergence of the series of modes), they do not appreciably affect the numerical values of the solution. Numerical results show that only a few higher order modes need be considered for good accuracy. It is physically reasonable to expect that since the modes of very high order are far beyond cutoff, they can have little physical effect.

It is not necessary to consider higher order modes at a boundary between a magnetic material and a nonmagnetic metal because the boundary conditions are only on the electric field.

Two experimentally practical arrangements will be treated in detail. 1) In Fig. 1(c), region 1 is empty and 3 is filled with a nonmagnetic perfect conductor. 2) In Fig. 1(d), both regions 1 and 3 are empty. A third problem of interest is that in which regions 1 and 3 are both filled with a perfect conductor. This problem of a filled rectangular cavity has been treated by several authors [18], [19]. The problem of a slab of magnetic material partially filling a cavity has not been solved completely.

II. The Waveguide Modes

The TE_{NO} modes in a lossless rectangular waveguide completely filled with transversely magnetized material can be written as follows.[2] (The h_z's do not enter into the solution and are thus not written down.)

$$e_y^n = A_n \sin n\nu \exp(\mp j\gamma_n z) \tag{1}$$

$$h_x^n = (\mp\zeta\gamma_n A_n \sin n\nu - \xi A_n \cos n\nu) \exp(\mp j\gamma_n z) \tag{2}$$

where

$$\nu \equiv \pi x/a$$
$$\gamma_n^2 \equiv \omega^2\mu_0\epsilon\mu_{eff} - (n\pi/a)^2$$
$$\zeta \equiv 1/\omega\mu_0\mu_{eff}$$
$$\xi \equiv (\pi/a)(\kappa/\mu)\zeta$$
$$\mu \equiv \mu_0(1+\chi)$$
$$\mu_{eff} \equiv [(1+\chi)^2 - \kappa^2]/(1+\chi)$$
$$a = \text{broad dimension of the waveguide.}$$

The permeability tensor has the Polder form

$$\mu = \mu_0(1+\chi) = \mu_0 \begin{bmatrix} 1+\chi & -j\kappa & 0 \\ 0 & 1 & 0 \\ j\kappa & 0 & 1+\chi \end{bmatrix}. \tag{3}$$

All fields are assumed to have an $\exp(j\omega t)$ time dependence.

III. Slab Against a Metal Wall

The analysis of this problem is somewhat less complicated than that of a slab with empty waveguide on both sides and, therefore, will be discussed first. The problem is diagramed in Fig. 1(c).

The applicable boundary conditions are

$$e_y^I + e_y^R = e_y^F + e_y^G \tag{4a}$$
$$h_z^I + h_z^R = h_z^F + h_z^G, \qquad z = -l \tag{4b}$$
$$e_y^F + e_y^G = 0, \qquad z = 0. \tag{4c}$$

Since there are no boundary conditions on the h_z's, we do not consider them here. For the sake of generality, we shall assume that the incident wave I consists of all TE_{NO} modes with known amplitudes I_m. Use of (1) and (2) along with similar expressions for the modes in empty waveguide [20] leads to the following expressions for the fields.

$$\begin{aligned}
e_y^I &= \sum_m I_m \sin m\nu \exp(-j\beta_m z) \\
h_z^I &= -\sum_m \zeta_m I_m \sin m\nu \exp(-j\beta_m z) \\
e_y^R &= \sum_p R_p \sin p\nu \exp(+j\beta_p z) \\
h_z^R &= -\sum_p \zeta_p R_p \sin p\nu \exp(+j\beta_p z) \\
e_y^F &= \sum_r F_r \sin r\nu \exp(-j\gamma_r z) \\
h_z^F &= -\sum_r F_r(\zeta\gamma_r \sin r\nu + \xi\cos r\nu) \exp(-j\gamma_r z) \\
e_y^G &= \sum_s G_s \sin s\nu \exp(+j\gamma_s z) \\
h_z^G &= \sum_s G_s(\zeta\gamma_s \sin s\nu - \xi\cos s\nu) \exp(+j\gamma_s z)
\end{aligned} \tag{5}$$

[1] See Gurevich [1], p. 193 ff.
[2] See Gurevich [1], ch. 9.

where

$$\beta_i^2 \equiv \omega^2\mu_0\epsilon_0 - (n\pi/a)^2$$
$$\gamma_i^2 \equiv \omega^2\mu_0\epsilon\mu_{eff} - (n\pi/a)^2$$
$$g_i \equiv \beta_i/\omega\mu_0.$$

The coefficients I_i, R_i, F_i, and G_i are the amplitudes of the ith mode of the wave described in Fig. 1(c). These expressions for the fields are to be inserted into the boundary conditions (4). It is convenient to introduce the operator Q_n, such that

$$Q_n f(v) \equiv (2/\pi)\int_0^\pi dv f(v)\sin nv, \tag{6}$$

which has the properties

$$\begin{aligned} Q_n \sin mv &= \delta_{nm} \\ Q_n \cos mv &= 0, \quad n = m \\ &= (2/\pi)[1 - (-1)^{n+m}]nm/(n^2 - m^2), \quad n \neq m \\ &\equiv M_{nm}. \end{aligned} \tag{7}$$

Operation on the boundary condition equations (4) with Q_n yields three sets of linear equations in the unknowns R_n, F_n, and G_n which are valid for all n.

$$\begin{aligned} I_n \exp(+j\beta_n l) - R_n \exp(-j\beta_n l) &= F_n \exp(+j\gamma_n l) \\ &\quad + G_n \exp(-j\gamma_n l) \end{aligned} \tag{8a}$$

$$\begin{aligned} &- g_n I_n \exp(+j\beta_n l) - g_n \exp(-j\beta_n l) \\ &= F_n(-\zeta\gamma_n \exp(+j\gamma_n l) - \xi\sum_q M_{nq}F_q \exp(+j\gamma_q l) \end{aligned} \tag{8b}$$

$$+ G_n\zeta\gamma_n \exp(-j\gamma_n l) - \xi\sum_q M_{nq}G_q \exp(-j\gamma_q l)$$

$$F_n + G_n = 0. \tag{8c}$$

If (8c) is used in (8a) and (8b), and if (8a) is then added to $(-1/g_n)$ times (8b), use of the definition

$$J_n^{\pm} \equiv \exp(+j\gamma_n l) \pm \exp(-j\gamma_n l) \tag{9}$$

leads to the set of linear inhomogeneous equations

$$\begin{aligned} 2I_n \exp(+j\beta_n l) &= F_n J_n^- + \zeta\gamma_n F_n J_n^+/g_n \\ &\quad + (\xi/g_n)\sum_q M_{nq}F_q J_q^-. \end{aligned} \tag{10}$$

This equation can be written in the form

$$P_n = \sum X_{nj}F_j \tag{11}$$

where

$$P_n = 2I_n(g_n/\xi)\exp(+j\beta_n l) \tag{12}$$

$$X_{nj} = M_{nj}J_j^- + \delta_{nj}(g_j J_j^- + \zeta\gamma_j J_j^+)/\xi. \tag{13}$$

The P_n's represent components of a known input vector. The elements of X_{nj} are also known. If it is desired to include the first L modes, then (11) represents a system of L linear inhomogeneous equations in the L unknown amplitudes F_j. The solution of this set of equations is readily accomplished by means of the Gauss–Jordan elimination technique [21] using a computer if values for χ and κ are available. The Gauss–Jordan technique with "pivoting" is very effective when the matrices are nearly singular. Once (11) has been inverted and values for the F_j have been obtained, the other required amplitudes can be easily derived from (8a) and (8c). Such solutions have been obtained and are discussed in detail in the following.

IV. Slab in Empty Waveguide

This problem is solved in a manner very similar to that in the previous section. The problem is diagramed in Fig. 1(d). The waves may be represented in the same manner as given in (5) with the addition of the transmitted wave T.

$$\begin{aligned} e_y^T &= \sum_i T_i \sin iv \exp(-j\beta_i z) \\ h_x^T &= -\sum_i g_i T_i \sin iv \exp(-j\beta_i z). \end{aligned} \tag{14}$$

The boundary conditions are (4a) and (4b) plus

$$\begin{aligned} e_y^T &= e_y^F + e_y^G \\ h_x^T &= h_x^F + h_x^G, \qquad z = +l. \end{aligned} \tag{15}$$

If we put the representations of the wave components (5) and (14) into the boundary conditions (15) and operate on all equations with Q_n we obtain the following equations.

$$\begin{aligned} I_n \exp(+j\beta_n l) &- R_n \exp(-j\beta_n l) \\ &= F_n \exp(+j\gamma_n l) + G_n \exp(-j\gamma_n l) \end{aligned} \tag{16}$$

$$\begin{aligned} &- g_n I_n \exp(+j\beta_n l) - g_n R_n \exp(-j\beta_n l) \\ &= -\zeta\gamma_n[F_n \exp(+j\gamma_n l) - G_n \exp(-j\gamma_n l)] \\ &\quad - \xi\sum_q M_{nq}[F_q \exp(+j\gamma_q l) + G_q \exp(-j\gamma_q l)] \end{aligned} \tag{17}$$

$$T_n \exp(-j\beta_n l) = F_n \exp(-j\gamma_n l) + G_n \exp(+j\gamma_n l) \tag{18}$$

$$\begin{aligned} &- g_n T_n \exp(-j\beta_n l) \\ &= -\zeta\gamma_n[F_n \exp(-j\gamma_n l) - G_n \exp(+j\gamma_n l)] \\ &\quad - \xi\sum_q M_{nq}[F_q \exp(-j\gamma_q l) + G_q \exp(+j\gamma_q l)]. \end{aligned} \tag{19}$$

We now introduce the following quantities.

$$\begin{aligned} c_n &\equiv \cos\gamma_n l \\ d_n &\equiv j\sin\gamma_n l \\ \mu_n &\equiv \zeta\gamma_n/g_n \\ \nu_n &\equiv \xi/g_n \\ \sigma_n &\equiv (1 + \mu_n)/\nu_n \\ \tau_n &\equiv (1 - \mu_n)/\nu_n \\ W_n &= 2I_n \exp(+j\beta_n l)/\nu_n. \end{aligned} \tag{20}$$

The coefficients R_n and T_n can be easily eliminated from (16) through (19), by multiplying (17) and (19) by $(-1/g_n)$ and adding and subtracting (16) and (17) and (18) and (19). Then the four equations, (16) through (19), reduce to two sets of equations in the F_n's and G_n's.

$$W_n = c_n(F_n\sigma_n + G_n\tau_n) + d_n(F_n\sigma_n - G_n\tau_n) + \sum_q M_{nq}[c_q(F_q + G_q) + d_q(F_q - G_q)] \tag{21}$$

$$0 = c_n(F_n\tau_n + G_n\sigma_n) - d_n(F_n\tau_n - G_n\sigma_n) - \sum_q M_{nq}[c_q(F_q + G_q) - d_q(F_q - G_q)]. \tag{22}$$

Let

$$A_n \equiv F_n + G_n$$
$$B_n \equiv F_n - G_n. \tag{23}$$

Addition and subtraction of (21) and (22) yields

$$W_n = Y_nA_n + 2\sum_q M_{nq}d_qB_q \tag{24}$$

$$W_n = Z_nB_n + 2\sum_q M_{nq}c_qA_q \tag{25}$$

where

$$Y_n = \rho_n(1 + \chi)\mu_{eff}[c_n + \gamma_n d_n/\mu_{eff}\beta_n]$$
$$Z_n = \rho_n(1 + \chi)\mu_{eff}[d_n + \gamma_n c_n/\mu_{eff}\beta_n] \tag{26}$$
$$\rho_n = 2\beta_n a/\kappa.$$

Again, if L modes are to be considered, (24) and (25) constitute a set of $2L$ linear inhomogeneous equations in the $2L$ unknowns A_n and B_n. As in the previous case, these equations can be solved by Gauss–Jordan reduction on a computer. The solutions for A_n and B_n yield values for F_n and G_n via (23). These values for F_n and G_n may be used in (16) and (18) to obtain R_n and T_n, respectively. The computed results of such solutions are discussed in the following.

V. RF Susceptibilities

Before numerical results can be obtained for either of these cases, values of the RF susceptibilities must be computed. Because some experimental data was available for comparison, the case of a two-sublattice easy-axis antiferromagnet at zero temperature with easy-axis aligned parallel to the applied dc magnetic field has been used.

The derivation of the RF susceptibilities, including loss, of a simple antiferromagnetic is well known, but complicated, because of the interaction of the two sublattices [23], [24]. The RF susceptibilities of an antiferromagnet are basically similar to those of a ferromagnet. MnF_2, a well-studied antigerromagnet, is employed.

Antiferromagnets, rather than ferrites, are treated here for several reasons. Foremost is that the author was studying antiferromagnetic resonance in MnF_2 when this problem was suggested. Thus, experimental data was available. Antiferromagnets are not so well-studied as ferrites, but are in many ways simpler to analyze [22], [23] and at low temperatures, at least, have a rather simple resonance which can be compared with the theoretical calculations. Although similar calculations and experiments on ferrites would be of real interest, the author has been unable to undertake them. The mathematical analysis is the same, except for susceptibility calculations which may be more difficult for ferrites.

VI. Results

Use of these RF susceptibility values enables one to compute the actual microwave field amplitudes and associated powers. In order to conform to the usual experimental situation, we take the incident wave to be purely TE_{10}.

For the case of a slab against a metal wall, we compute the reflected power. For the slab in empty waveguide we compute the reflected, transmitted, and absorbed powers. Fig. 2 shows the power reflected from a slab of antiferromagnetic MnF_2 against a metal wall as a function of applied field in the vicinity of the resonance. Fig. 3 shows the reflected, transmitted, and absorbed powers for a slab in open waveguide computed for an antiferromagnet.

Analysis of these theoretical results shows that if the incident wave is purely TE_{10}, only the first few higher order modes need be considered. Calculations including four modes gave essentially the same results as calculations including ten modes. Analysis shows further that the mode content of the incident wave does not significantly affect the relative amounts of energy reflected and transmitted. The mode content does, of course, change.

In order to check on the usefulness of this rather involved analysis, a calculation based on a plane-wave approximation to the problem of a slab in empty waveguide was performed.[3] In Fig. 4, experimental measurements of the energy transmitted through a slab of antiferromagnetic MnF_2 [25] are compared with both the exact solution treated previously and with the plane-wave approximation. Both theoretical curves were fitted to the experimental data with the use of only one adjustable parameter, the resonance linewidth. The magnitude of the drop in transmitted energy as the sample passes through resonance is not adjusted. The same values for χ and κ were used in both calculations. Fig. 4 shows clearly that the results of the calculation presented in this paper are in much closer agreement with experimental data than are the results of the plane-wave approximation.

The experimental data shown in Fig. 4 was taken with longitudinal magnetization. It has been found that the theoretical calculation presented here fits experimental

[3] See Gurevich [1], ch. 7.

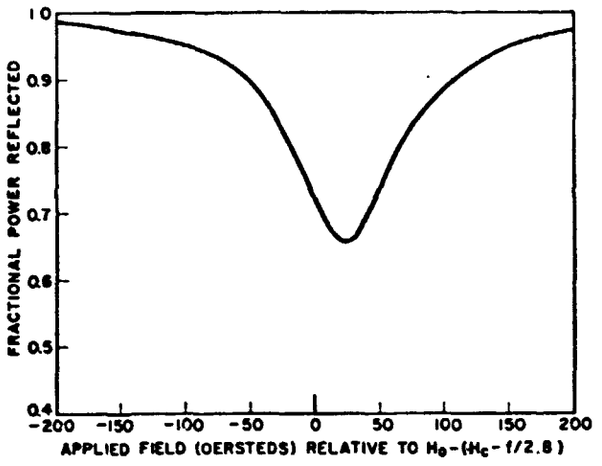

Fig. 2. Computed curve of antiferromagnetic slab in shorted *RG* 98 waveguide. Frequency = 270.8 GHz, $\Delta H = 0.009T$, thickness = 0.3 mm.

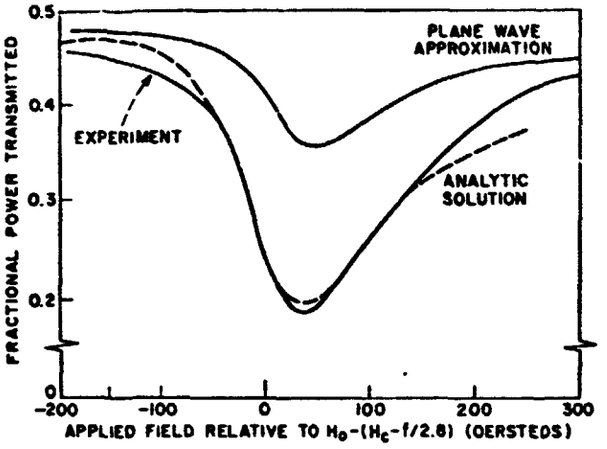

Fig. 3. Computed curves of antiferromagnetic slab in open *RG* 98 waveguide. Frequency = 250 GHz, $\Delta H = 0.0090T$, thickness = 0.63 mm.

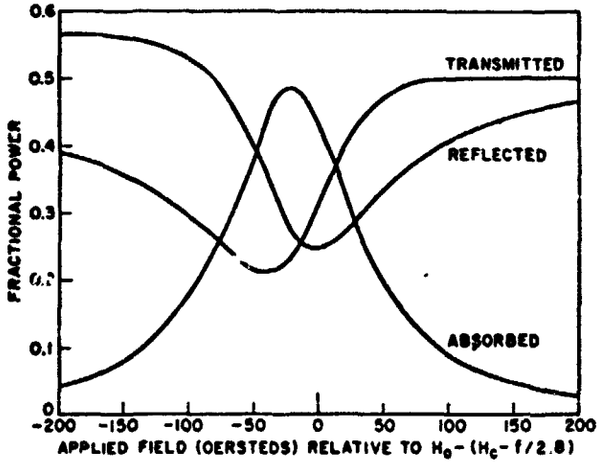

Fig. 4. Comparison of experimental data with analytic solution and with plane-wave approximation of antiferromagnetic slab in open *RG* 98 waveguide. Same conditions as in Fig. 3.

data on thin MnF_2 slabs equally well for both longitudinal and transverse magnetizations. Due to the fact that the modes in the sample are quite different for the two cases [1], this is rather surprising and no satisfactory explanation has been offered. A clue to the resolution of this issue is that the computed amplitudes of the higher order modes generated at the interface are very small for MnF_2. Further, the fact that the samples were very thin should mitigate the effect of any other types of modes. The solution to the same problem for longitudinal magnetization is forbiddingly difficult and has not been attempted.

Gagné [24] and others have discussed the existence of surface modes which might propagate through cracks left between the sample and the waveguide wall. In these experiments care, but not special care, was taken to insure a good fit. The fact that the theoretical results fit experimental data rather well without assuming the existence of crack modes may be in conflict with Gagné's result. On the other hand, his measurements were on ferrites which have much higher permeabilities than antiferromagnets and his samples had an electrical thickness of roughly one wavelength, rather than one-tenth wavelength used here. Extension of my calculations and experiments [25] to thick samples (greater than one-half wavelength) shows that very complicated dimensional resonances occur in thick samples, even without assuming the existence of crack modes. This work then, neither confirms nor denies such modes.

In order to justify the technique presented here, some comments should be made on mathematical difficulties. Discussions of the air–ferrite interface by Mittra and Lee [26] and their references are relevant here because the permeability tensor and, thus, the waveguide modes are the same for an antiferromagnet as for a ferrite.

Mittra and Lee actually treat a substantially different problem in that they invoke a quasi-static approximation and do not include losses. The solutions presented here are exact. Only in the numerical analysis are approximations used where the coefficient matrix is truncated at finite order. Nonetheless, it is useful to consider possible homogeneous solutions to (10) or (24) and (25). The antisymmetric matrix formed by the $M_{n,n+1}$ increases without bound as n increases. Further, if the matrix is truncated for L odd, it is singular. It is convenient to look at the semi-infinite case [17]. The equation corresponding to (10), (24), and (25) is

$$2g_n I_n = \xi \sum_q [M_{nq} + (g_q + \zeta\gamma_q)\delta_{nq}/\xi] T_q \qquad (27)$$

where the T_q are the transmitted amplitudes. If the I_n are all zero, a nontrivial solution will exist for the T_q only if the coefficient determinant is zero. As an example, consider the case $L = 1$. Equation (27) then becomes (all I_n's are zero)

$$T_1(g_1 + \zeta\gamma_1)/\xi = 0.$$

if T_1 is to be zero, we must have

$$\frac{g_1}{\xi} + \frac{\zeta\gamma_1}{\xi} = 0$$

which means either 1) $\xi \to \infty$ or 2) $g_1 + \zeta\gamma_1 = 0$.

Case 1:

$$\xi = (\pi/a)(\kappa/\mu)[\mu/\omega\mu_0(\mu^2 - \kappa^2)]$$

$$\xi \sim \frac{\kappa}{\mu^2 - \kappa^2} \to \infty. \tag{28a}$$

Case 2:

$$g_1 + \zeta\gamma_1 = 0$$

$$[\omega^2\mu_0\epsilon_0 - (n\pi/a)^2]^{1/2}/\omega\mu_0 + [\omega^2\mu_0\epsilon\mu_{eff} - (n\pi/a^2)]^{1/2}/\omega\mu_0\mu_{eff} = 0. \tag{28b}$$

If loss is not included in μ and κ, they are both real and it is clear that either (28a) or (28b) might hold. On the other hand, simple manipulation of (28a) and (28b) for complex μ and κ shows that neither condition can hold. Similar analysis for larger values of L shows that no homogeneous solutions are possible so long as μ and κ are complex. The inclusion of loss then actually simplifies the problem, as well as introducing more physical significance.

It is important to emphasize that the electrodynamic analyses presented here are valid for any material with the assumed properties. This fact is useful because susceptibility calculations based on any model can be directly compared with experimental results, since the analysis is independent of the model used for susceptibility calculations. Exact solutions typically allow experimental data to be fitted to theory, not only with more accuracy, but often with fewer adjustable parameters. For example, Fig. 4 shows that the plane-wave solution gives the position and shape of the resonance rather well but tells little about the magnitude of the effects. The waveguide solution, however, also gives the magnitude. Typically, the susceptibilities of the material depend on several parameters which may require several different experiments or often different types of experiments to determine. If one experimental measurement can yield additional information about these parameters—even only one additional value—an entire experiment might be avoided. The work involved in this rather complex theoretical analysis would often be much less than that involved in such an experiment.

In the past, many measurements of the microwave properties of magnetic materials have been made on very small samples in microwave cavities because perturbation theory calculations work fairly well for that case. The availability of these exact solutions for samples in a waveguide now offers the experimentalist the alternative of making measurements on relatively large samples in standard waveguide, and thus, avoiding the experimental difficulties associated with very small samples and microwave cavities. Measurement of phase shift and absorption can be made much more quickly and easily by waveguide transmission or reflection techniques than by means of measuring changes in cavity Q and resonant frequency. Experimental data can be matched to specific values of the RF susceptibilities through the medium of a curve fitting computer program based on the calculations described previously. Such values of the susceptibilities would be useful in many device design calculations. This approach to the measurement of microwave properties of magnetic materials should be especially useful for studies of frequency dependence and for measurements at millimeter wavelengths.

Acknowledgment

The author extends his gratitude to Prof. G. S. Heller, who supervised this research, and to Prof. D. M. Bolle, who lent considerable theoretical assistance. I. M. Besieris and C. P. Wu made many useful suggestions.

References

[1] A. G. Gurevich, *Ferrites at Microwave Frequencies*. New York: Consultants Bureau, 1963. Especially chs. 6–9.
[2] B. Lax and K. J. Button, *Microwave Ferrites and Ferrimagnetics*. New York: McGraw-Hill, 1962. Especially chs. 7–9.
[3] D. Polder, "On the theory of ferromagnetic resonance," *Phil. Mag.*, vol. 40, p. 99, 1949.
[4] A. A. T. Van Trier, "Guided electromagnetic waves in anisotropic media," *Appl. Sci. Res., Sect. B*, vol. 3, pp. 305–370, 1953.
[5] M. L. Kales, "Modes in waveguides containing ferrites," *J. Appl. Phys.*, vol. 24, pp. 602–608, May 1953.
[6] P. S. Epstein, "Theory of wave propagation in a gyrotropic medium," *Rev. Mod. Phys.*, vol. 28, pp. 3–17, January 1956.
[7] P. H. Vartanian and E. T. Jaynes, "Propagation in ferrite-filled transversely magnetized waveguide," *IRE Trans. Microwave Theory and Techniques*, vol. MTT-6, pp. 140–143, July 1956.
[8] D. J. Angelakos and M. M. Korman, "Radiation from ferrite-filled rtures," *Proc. IRE*, vol. 44, pp. 1463–1468, October 1956.
[9] M. L. Seavey and P. E. Tannenwald, "Electromagnetic propagation effects in ferromagnetic resonances," M.I.T. Lincoln Laboratory, Lexington, Mass., Tech. Rept. 143, 1957.
[10] C. B. Sharp and D. S. Heim, "A ferrite boundary—value problem in a rectangular waveguide," *IRE Trans. Microwave Theory and Techniques*, vol. MTT-6, pp. 42–46, January 1958.
[11] P. S. Epstein, *Usp. Fiz. Nauk.*, vol. 65, p. 283, 1958.
[12] G. Tyras and G. Held, "Radiation from a rectangular waveguide filled with ferrite," *IRE Trans. Microwave Theory and Techniques*, vol. MTT-6, pp. 268–277, July 1958.
[13] A. D. Bresler, "On the discontinuity problem at the input to an anisotropic waveguide," *IRE Trans. Antennas and Propagation*, vol. AP-7, pp. S261–S272, December 1959.
[14] M. E. Brodwin and D. A. Miller, "Propagation of the quasi-TEM mode in ferrite-filled coaxial line," *IEEE Trans. Microwave Theory and Techniques*, vol. MTT-12, pp. 496–503, September 1964.
[15] F. J. Rosenbaum, "Electromagnetic wave propagation in lossy ferrites," *IEEE Trans. Microwave Theory and Techniques*, vol. MTT-12, pp. 517–528, September 1964.
[16] R. Mittra and S. W. Lee, "Discontinuity problem in an anisotropic waveguide," *J. Appl. Phys.*, vol. 38, pp. 3178–3184, July 1967.
[17] K. C. O'Brien, "Microwave properties of a rectangular waveguide semi-infinitely filled with magnetic material," this issue, pp. 400–402. Additional references are given in this paper.
[18] G. S. Heller, "Ferrite-loaded cavity resonators," *Proc. Internatl. Congress on UHF Circuits and Antennas, Onde Elect.*, Special Suppl. vol. 2, p. 588, October 1957.
[19] D. M. Bolle, *Electron. Letters.*, vol. 2, p. 1, January 1966.
[20] R. E. Collin, *Foundations of Microwave Engineering*. New York: McGraw-Hill, 1966, p. 102.
[21] See any text in numerical analysis.
[22] F. Keffer and C. Kittel, "Theory of antiferromagnetic resonance," *Phys. Rev.*, vol. 85, p. 329, January 1952.
[23] G. S. Heller *et al.*, "Antiferromagnetic materials for millimeter and submillimeter devices," *J. Appl. Phys.*, vol. 32, Suppl. 3, p. 307S, March 1961.
[24] R. R. J. Gagné, "The paradoxical surface wave (crack wave) in ferrite-filled waveguides," *IEEE Trans. Microwave Theory and Techniques*, vol. MTT-16, pp. 241–250, April 1968.
[25] K. C. O'Brien, "The effects of size, shape and frequency on the antiferromagnetic resonance line width of MnF_2," *J. Appl. Phys.*, to be published.